A revisitation of the triangular prism surface area method for estimating the fractal dimension of fractal surfaces

Angelo De Santis([1]), **Maurizio Fedi**([2]) **and Tatiana Quarta**([3])
([1]) *Istituto Nazionale di Geofisica, Roma, Italy*
([2]) *Dipartimento di Geofisica e Vulcanologia, Università «Federico II», Napoli, Italy*
([3]) *Dipartimento di Scienza dei Materiali, Università di Lecce, Italy*

Abstract
Fractal dimension is widely used to give a measure of variability and roughness of curves, signals, objects, statistical distributions, and so on. We found that an often used method, the so-called triangular prism surface-area method, for estimating the fractal dimension of fractal surfaces possesses some intrinsic mistakes in application. This note describes the misinterpretation and suggests the proper application, that we call Revised Triangular Prism Method (RTPM). To show its feasibility we apply RTPM to some synthetic Euclidean and fractal surfaces of known dimension.

Key words *fractal dimension – self-affinity – self-similarity – triangulation*

1. Introduction

Everywhere Nature gives so many examples of fractals that scientists finally realised that fractal geometry can be of great utility to measure, classify and/or represent some properties of objects, ensembles, or curves.

Estimating the fractal dimension is not a simple problem, also because it is related to the intrinsic difficulty to strictly define a fractal. No clear and self-consistent definition really exists. According to Mandelbrot, a fractal is «a set for which the Hausdorff-Besicovitch dimension D strictly exceeds the topological dimension d» (Mandelbrot, 1983; p. 15). For Russ (1994) fractals occupy a borderline between Euclidean geometry and complete randomness, whilst Kaye (1994), reviewing Russ' book, more simply considers them as structures of rugged systems.

Many standard algorithms have been developed for estimating the fractal dimension of one-dimensional irregular curves. Some have been proposed by Mandelbrot (1983) as ruler-method (named also Mandelbrot-Richardson Method), length-area relations (that Mandelbrot extends also to volumes), and box-counting methods. In particular, the former is essentially based on the introduction of fractals with the classic example of estimating the length of a coastline (Mandelbrot, 1967). These are essentially methods for *self-similar* fractals, *i.e.* for curves with same units and same scaling of variations along the two axes of the plane (in contrast with *self-affine* fractals where units and/or scalings are different). Other methods like the *rescaled range* (*e.g.*, Mandelbrot and Wallis, 1969), the variogram (*e.g.*, Herzfeld *et al.*, 1993) and the spectral methods (*e.g.*, Hough, 1989) allow us to compute the fractal

Mailing address: Dr. Angelo De Santis, Istituto Nazionale di Geofisica, Via di Vigna Murata 605, 00143 Roma, Italy; e-mail: desantisag@ing750.ingrm.it

dimension also for *self-affine* fractals. Dubuc *et al.* (1989) describe these and other one-dimensional methods. Carr and Benzer (1991) and Carr (1995; p. 512) show some cautions in comparing the ruler method with the spectral and variogram methods, affirming that the former yields a fractal dimension which is a measure of complexity of shape, while the latter indicate similarity of the fractal curve to noise. In our opinion, the most substantial difference is that the *self-similar* methods (like the ruler method) are sensitive to both the horizontal and the vertical variations, while the *self-affine* methods depend only on vertical variations. In other words, stretching or compressing a self-affine curve does not change its affinity dimension while a self-similar curve changes its characteristic roughness and its similarity dimension.

When we pass to analyse the fractal dimension of fractal surfaces, the difficulties increase. According to Feder (1988; p. 215): «the question of how to deal properly with fractal surfaces in practice has not been completely resolved». However, the variogram and the spectral methods, appropriately generalised (*e.g.*, see Turcotte, 1992), can be applied. Another method which is often used is the so-called *triangular prism surface area* method or, more briefly, the Triangular Prism Method (TPM). This method strictly furnishes an estimate of the fractal dimension of fractal self-similar surfaces; nevertheless, it can be applied to self-affine surfaces providing an objective and quantitative measure of irregularity and roughness classification.

This note is a remark on some systematic mistakes which have normally been made when this particular method was applied. We will describe the revised TPM and its proper application to some synthetic cases. The appendices A, B and C will be the necessary basis for the next sections.

2. Triangular prism method

Although the method of triangulation to estimate a surface area is rather old, in recent times for specific *fractal* purposes, Clarke (1986) introduced the current version of TPM that was then applied also by other authors, even recently (*e.g.*, Jaggi *et al.*, 1993). This method is called the *patchwork* method by Roach and Fowler (1993). The TPM is considered the two-dimensional extension of the ruler method (*e.g.*, Korvin, 1992, pp. 175-177), where the surface ruler is the upper surface of a series of triangular prisms. Since in the one-dimensional case the fractal dimension is self-similar and called ruler or divider dimension, also here the fractal dimension provided by TPM is a self-similarity dimension and *not* a self-affine dimension. In this respect this method usually differs from self-affine techniques as the spectral and the variance methods which estimate the self-affine dimension.

Let us consider a digital representation of the fractal surface in the form of a square $n \times n$ ($= N$) grid with the elevations of the investigated surface as z-values of the grid. Then we may cover the surface with prisms of square bases s which are, in turn, divided into an even number of triangular prisms and then compute the area, for instance, by means of Heron's formula (*e.g.*, Clarke, 1986) or using vector algebra (Creutzburg and Ivanov, 1989). The use of even series of triangular prisms should avoid the occurrence of the so-called Schwarz paradox (*e.g.*, Korvin, 1992, pp. 245-249) where normal triangulation of simple geometrical surfaces like, for instance, cylinders, can give some absurd results (see Appendix B).

From a power-law relation between total area A and projected surface ruler $\sigma' = s^2$, Clarke (1986) provided a way to estimate the fractal dimension of the surface. The method has been applied to topographic grids (Clarke, 1986), remote-sensing data (Jaggi *et al.*, 1993) and image segments (Creutzburg and Ivanov, 1989). In practice the evaluation of the fractal dimension (with D in the range 2 to 3) is made estimating the slope β' in a plot with the logarithm of the total surface as y-axis and the logarithm of the so-called surface *tile* as x-axis. The tile is the unit area σ' used each time as surface ruler. The value of D is estimated as $2 - \beta'$ (Clarke, 1986).

In the present application of TPM we disclose two specific problems that involved corresponding misinterpretations.

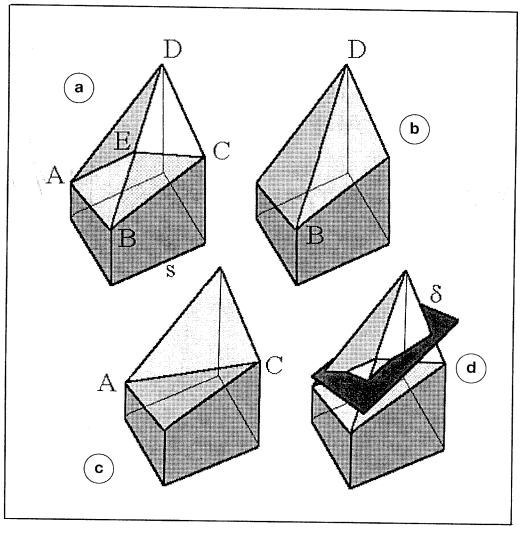

Fig. 1a-d. Possible elementary prisms used to cover the investigated surface. a) Upper surface divided in 4 triangles, with mean elevation as common central point E: common application of the Triangular Prism Method (TPM; Clarke, 1986). b), c) Upper surface divided in two triangles (*e.g.*, Piech and Piech, 1990). To distinguish (a) from (b) and (c) we called the former TPM4 and the latter two TPM2, in accordance with the number of triangles used to compute the area of the i_{th} prism. d) We introduce a virtual square with area σ_i equal to the area computed with TPM4 and side $\delta_i = \sqrt{\sigma_i}$; the mean square σ among the all σ_i covering the surface is the area tile considered in this paper for the revised triangular prism method (RTPM).

Before describing these two points it is important to refer to the question of the possibly different coverages of the surface under study. The common procedure of TPM is to consider four experimental points at a time forming a quadruple. The quadruple can be either covered i) by 4 triangles with mean elevation of the four vertices as a common central point (fig. 1a; *cf.* Clarke, 1986), or ii) by just 2 triangles (fig. 1b,c; *cf.* Piech and Piech, 1990). To distinguish the two approaches, we now call methods i) and ii) with TPM4 and TPM2, respectively, where the final number indicates the number of triangles used to split the top surface of each quadruple. It is easy to demonstrate that, in general, the two coverages (fig. 1b,c) of TPM2 give very similar surface area estimations, but usually differ from the areas computed with TPM4. With some numerical tests, we found that most of the time, the TPM2 overestimates the expected areas, sometimes also significantly; this fact is more evident when the Euclidean surfaces contain abrupt discontinuities. For instance, this can be seen for the two Euclidean surfaces of fig. 2. Both cases show 65×65 grids where a cube (top; side = 32 units) or a half sphere (bottom; radius = 32 units) is placed at the centre of a horizontal base. In each example the true total surface area (indicated in the figure at the right of each object) is the combination of the upper surface of the geometrical object and the rest of the planar base to complete the 65×65 grid. Figure 2 also shows the corresponding total area estimations given by the two methods when the smaller tile is used. The values furnished by TPM2 are larger than the theoretical ones; this would imply, in case of subdivision as TPM2, an overestimation of the fractal dimension. Only TPM4 is significantly close to the true values. For this reason in the following, even if we call it simply TPM (or subsequently RTPM) we will always make use of the 4-triangle coverage of TPM4 (as in fig. 1a).

One of the two points that all previous works missed is that the small triangular tiles considered as surface rulers are not in a simple relation with the cross sections σ' (or corresponding sides s) of the base of the prisms, but also depend on the properties of the surface itself. In our following approach for the i_{th} prism, instead of the base cross section σ_i', we will consider a virtual square with side $\delta_i = \sqrt{\sigma_i}$ (fig. 1d) where σ_i is the real upper surface of the i_{th} prism (see Appendix B). Then we will assume $\delta = < \delta_i >$ as mean ruler. It is clear that δ is different from s used by previous authors.

The second point regards the improper formulation that previous authors used to determine D.

Following the theory expressed in Appendix A, we will apply it to the case of the TPM. Let us cover the fractal surface with N prisms of

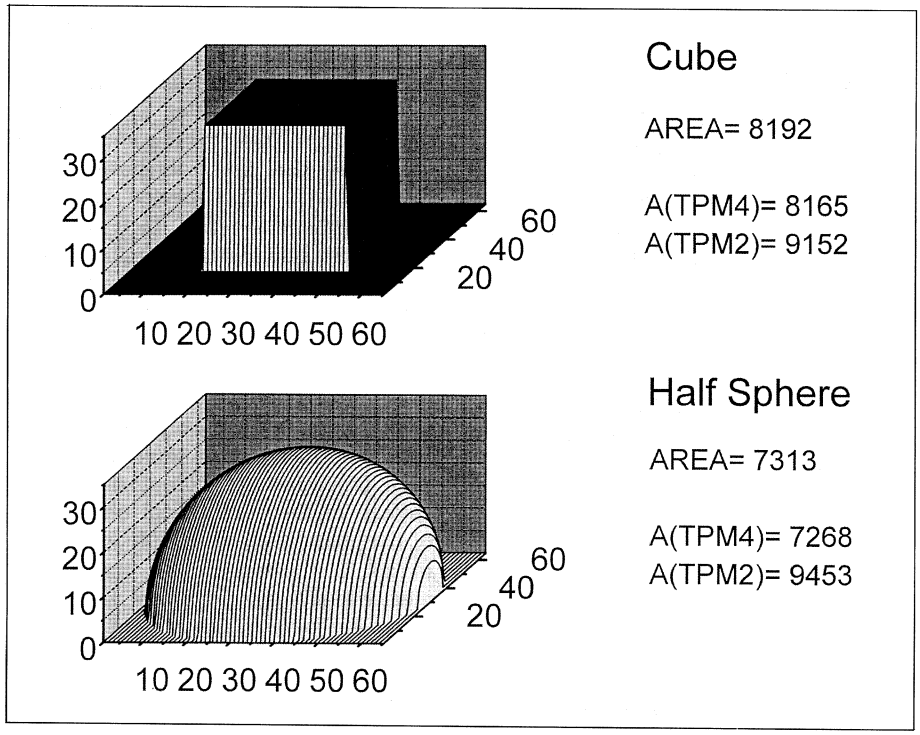

Fig. 2. Two examples of Euclidean surfaces (a 65×65 grid base with a cube or a half sphere) of given surface areas to test the methods TPM4 and TPM2. TPM4 provides better estimations of the surface areas while TPM2 has the tendency to overestimate them in cases with abrupt changes, as shown here where planar bases suddenly change to a cube or a half sphere. The cube and the half sphere have 32 units of side or radius, respectively. The surface areas include also the remaining base to complete the 65×65 grid.

mean upper surface $\sigma = \delta^2 = <\delta_i>^2$ (fig. 1d). For $\delta \to 0$, we can write (Appendices A and C):

$$A(\delta) \propto \delta^{(2-D)} = \delta^{\gamma} \qquad (2.1)$$

or, in terms of $\sigma = \delta^2$:

$$A(\sigma) \propto \sigma^{(2-D)/2} = \sigma^{\beta} \qquad (2.2)$$

for $\sigma \to 0$.

Equations (2.1) and (2.2) imply that the fractal dimension can be evaluated from the slope γ of the linear part of $\log A$ *vs.* $\log \delta$:

$$D = 2 - \gamma \qquad (2.3)$$

or from the slope β of the linear part of $\log A$ *vs.* $\log \sigma$ graph:

$$D = 2(1 - \beta) \qquad (2.4)$$

which are quite different from the relations given by Clarke (1986) and by Creutzburg and Ivanov (1989). We call the corrected way to apply TPM the Revised Triangular Prism Method (RTPM). Our expressions are also partly confirmed by Russ (1994; p. 61) for tessellation with equilateral triangles and by similar expressions shown by Korvin (1992; p. 245), although they do not mention the mistake explicitly. Piech and Piech (1990) use the correct relation (their eq. (3) at p. 465) among

$A(\delta)$, D and the ruler (the latter two called by Piech and Piech (1990) α and s respectively), but it is not completely clear which δ they actually used. Moreover, they applied the TPM2 which, as shown before, usually gives overestimated values of fractal dimension.

To make the results obtained by previous authors using original TPM more compatible with the equation (2.2), their estimations D' of the fractal dimension can be used to deduce a lower bound D_L of the correct D as:

$$D_L = 2(D' - 1). \qquad (2.5)$$

Note that D_L is a lower bound of the true dimension, *i.e.*, it is less than or equal to D, since $\delta > s \neq 0$.

3. Application to synthetic cases

To test and verify the RTPM, we synthesized some surfaces of known dimension (Euclidean or fractal surfaces) in 65×65 square grids. In particular, the Euclidean surfaces consisted of cylindrical surfaces of different sizes (lower left of fig. 3 shows an example; we chose this particular kind of surfaces to numerically check that the Schwarz paradox did not occur) and the 2D function:

$$z(x,y) = y \cos(\pi x/40)$$

(upper left of fig. 3). On the other hand, the fractal surfaces were expressed as Weierstrass-

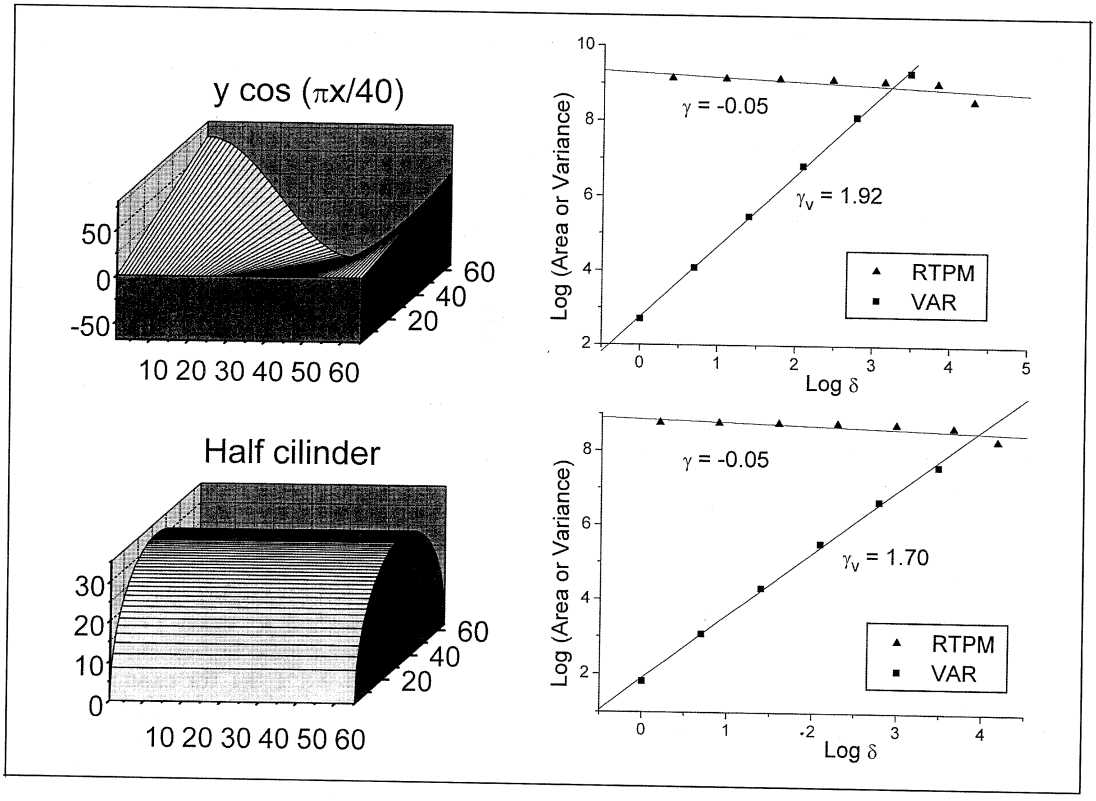

Fig. 3. Examples of fractal dimension estimation for Euclidean surfaces (lower left: half cylinder with height $H = 64$ and radius $R = 32$ units; upper left: $y \cos(\pi x/40)$ with RTPM and variance method. Graphs at the right are the corresponding generalised Richardson-Mandelbrot plots.

Mandelbrot (WM) functions $W(x,y)$ of the following form:

$$W(x, y) =$$

$$= K \sum_{j=ja,\, jb} \frac{\cos(\sqrt{2}\pi b^j x + \alpha_j)\cos(\sqrt{2}\pi b^j y + \phi_j)}{b^{(3-D_a)j}} \tag{3.1}$$

where α_j and ϕ_j are pre-chosen (deterministic or random) phases and $b = 1.5$. K is a normalization constant and ja and jb should be theoretically $-\infty$ and ∞, respectively. $W(x,y)$ is a self-affine function with fractal self-affine dimension D_a comprised between 2 and 3. Unfortunately, since RTPM is a self-similar method, we cannot directly compare its fractal dimension D with D_a. We could scale the WM functions differently in accordance with their D_a; however this procedure could become particularly complicated. On the other hand, we recall that if the vertical profile of a random surface is self-similar with fractal dimension D_1 then the fractal dimension of the surface itself is $D_s = D_1 + 1$ (*e.g.*, Korvin, 1992; p. 256). This property will allow us to test the feasibility of our method. We produced many unidimensional 1024-point realizations of expression (3.1) at fixed x or y, using $ja = -16$ and $jb = -1$ as summation limits, in order to select significant samples of WM surfaces of given dimension D at steps of 0.1 between 2 and 3. These series of unidimensional functions were analysed with a divider technique (in particular that given by Russ, 1994) and the corresponding estimated fractal dimensions, D_1, increased by 1, were used to test the results given by RTPM when applied on the corresponding fractal WM surfaces. We found a one-to-one linear relation between D_s and D_a. Since RTPM is the two-dimensional version of the divider method, we would expect good agreement between the values of our method and those deduced from the unidimensional analyses.

Therefore we synthesized 9 series of random WM surfaces (*i.e.*, with random α_j and ϕ_j) such that $D_s = 2.1, 2.2, \ldots, 2.9$, normalising each function in order to let its larger z-deviation be the same as the larger horizontal extent (this was the rule applied by the 1-d divider technique). Figure 4 shows two examples with $D_s = 2.3$ and $D_s = 2.8$.

On the synthetic cases, we also applied another method called bidimensional variogram method or simply variance method (*e.g.*, Turcotte, 1992, chapter 7), in order to verify the self-affine dimension of each selected WM function. This method is based on the following relation between the variance of the experimental function $Z(x,y) = Z(\boldsymbol{x})$ and the corresponding fractal self-affine dimension D_a:

$$\frac{d\log < [Z(\boldsymbol{x}_0) - Z(\boldsymbol{x}-\boldsymbol{x}_0)]^2 >}{d\log \boldsymbol{x}} = 6 - 2D_a \tag{3.2}$$

which is the 2D extension of the 1D expression (*e.g.*, Korvin, 1992, p. 262).

In the following applications of the methods for estimating D we used the rulers: 1, 2, 4, 8, 16 and 32 units (we preferred to exclude the larger ruler of 64 units to avoid possible edge effects; see also Appendix B). Two generalised Richardson-Mandelbrot log-log plots are presented in fig. 4 at the right of the corresponding analysed surfaces. All results are summarized by fig. 5, where the errors have been estimated as the larger half deviation among the results of several cases (at least 5) for each D_s; the dashed line represents the theoretical expected relations for D_s or D_a. Within the errors, RTPM always agrees with $D_s = D_1 + 1$ while TPM, as introduced by Clarke (1986), provides lower values especially at higher values of true D. On the other hand, as expected, the variance method furnishes values close to the self-affine dimensions of the WM functions.

Further confirmation is given for the experimental images named as examples A and B by Clarke (1986). Applying the RTPM and the variance method to these 17×17 square matrices we found good agreement with similar values ($D = 2.8 \pm 0.1$ for example A and $D = 2.4 \pm 0.1$ for example B), although we used four rulers for RTPM and only three for the variance method. Since the variance method is for self-affine fractals, the coincidence of results between the two methods can be explained by an almost self-similarity of the two digitised images.

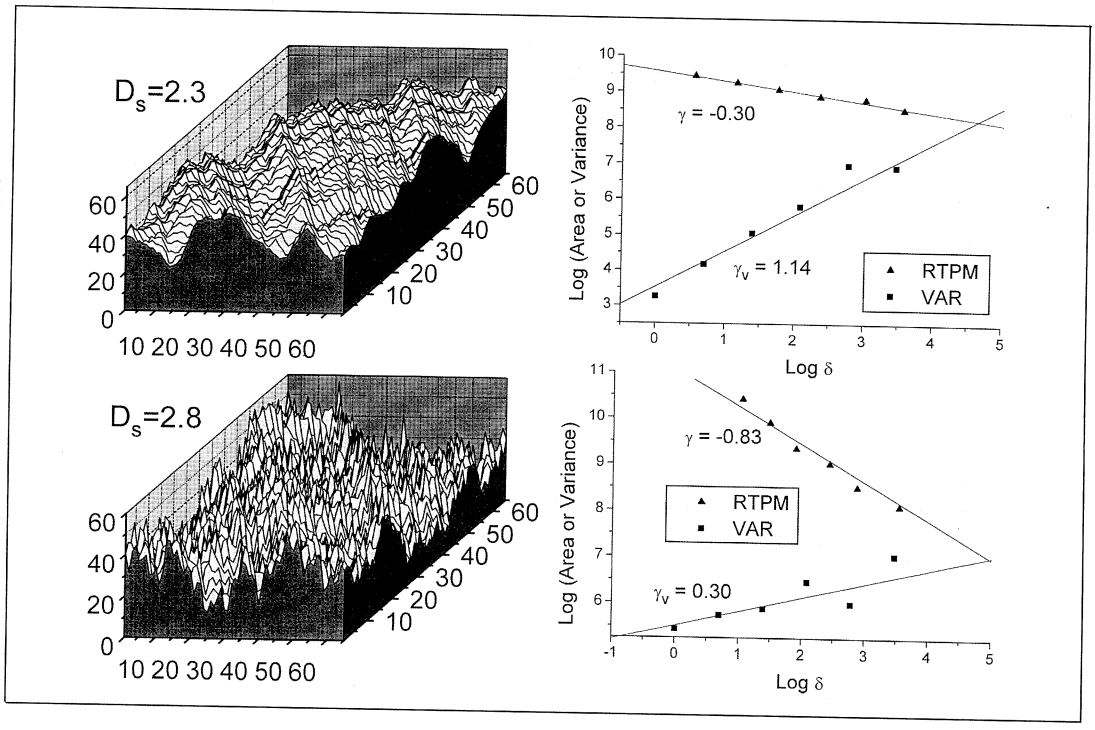

Fig. 4. As fig. 3 but for fractal surfaces: Weierstrass-Mandelbrot functions with $D_s = D_1 + 1 = 2.3$ (up) and 2.8 (bottom).

We cannot check our method RTPM directly on data of previous works which are not available to us, but the correction (2.5) would imply, for instance, that the example of Bell Canyon DEM of Clarke (1986; his fig. 5) possesses a value greater than 2.38 which seems more consistent with the rugged aspect of the digitised image. Even the recent work of Jaggi *et al.* (1993) presents the same misinterpretations as Clarke (1986) and Creutzburg and Ivanov (1989); this can also justify why their example with the uncorrected version of this method gives a rather low estimation for a fractal surface representing remotely sensed data (their value of 2.2 would change to another greater than 2.4).

As all fractal methods, also the RTPM must be used with some caution when applied to real data; careful investigation of the log-log plots is always necessary in order to clearly assess the possible fractality of the surface under study. Moreover, RTPM is typically for self-similar, monofractal and isotropic surfaces when real data are often self-affine fractals or multifractals (*e.g.*, Feder, 1988; chapter 6) and anisotropic, therefore the method provides the correct fractal surface dimension only for self-similar surfaces. Nevertheless, even in case of no self-similar surfaces, the results given by RTPM represent an objective measure of the tendency of the surface itself to occupy the volume at its disposal; this can be particularly useful when there is the need to classify surfaces belonging to the same homogeneous set of two-dimensional experimental data. Finally, there are also situations where, although the surfaces under study are probably self-affine, the divider technique is more suitable than other self-affine methods. This is, for example, the case of rock surfaces for which it has been

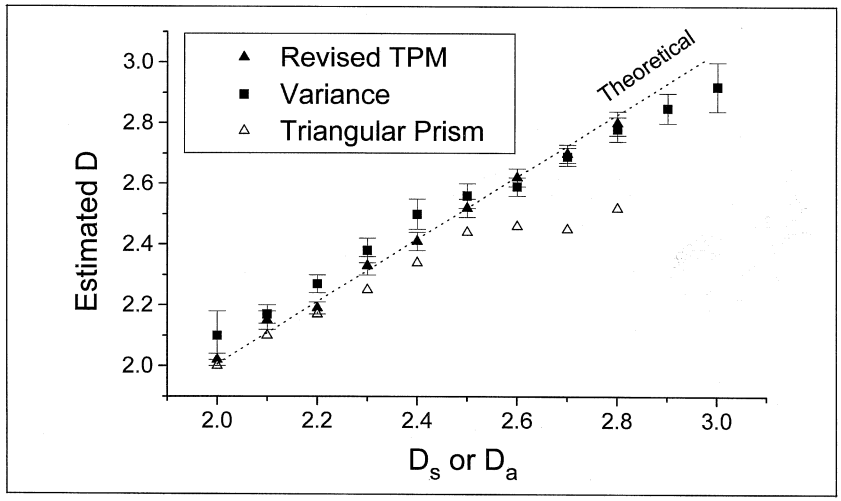

Fig. 5. Comparison of the RTPM, TPM and variance method for estimating fractal surface dimension. Dashed line represents the theoretical expected relations for D_s or D_a. Within the estimated errors, RTPM and Variance method provide always correct values. On the contrary, for high values of true D, TPM saturates at around 2.5. The errors have been estimated as the larger half deviation among the results of several cases (at least 5) for each D_s: in order to avoid confusion the errors associated with TPM have not been indicated, however they are of the same order of the corresponding RTPM case at the same D_s.

found that the fractal dimension provided by the divider technique is a better descriptor of their roughness, than the self-affine dimension (Carr, 1995, p. 518).

4. Conclusions

Generally, the triangular prism area method appears to be a reliable and reasonably fast method to compute the fractal dimension of fractal surfaces. The RTPM, as here applied, results in easier computer implementation and shorter computation time than other bidimensional fractal methods, especially if compared with variogram and spectral methods.

Systematic conceptual mistakes in: a) the use of the appropriate ruler; b) the kind of coverage and c) the basic relation between fractal dimension and slope of the log-log plot, regularly led to wrong results, most of the time lower than expected. In this note we have described the proper application, verified its potentiality on many synthetic surfaces and given also a simple way to define a lower bound of the true fractal dimension from results estimated by authors of previous works. The new assessment of the method may give further help when the evaluation of the surface fractal dimension is of vital importance. This is the specific case of geology and geophysics, where generally the fractal dimension has been estimated along the corresponding profiles instead of considering, more appropriately, the whole surfaces (*e.g.*, clouds and mountains, fractures and faults, topography and bathygraphy, etc.).

Acknowledgements

We thank K. C. Clarke, G. Korvin and J. W. Kruhl for their valuable suggestions and comments. One of the authors (ADS) thanks V. De Rubeis for the helpful discussions during some long traffic jams in Rome.

REFERENCES

CARR, J.R. (1995): *Numerical Analysis for the Geological Sciences* (Prentice Hall, New Jersey), pp. 592.

CARR, J.R. and W.B. BENZER (1991): On the practice of estimating fractal dimension, *Math. Geology*, **23** (7), 945-958.

CLARKE, K.C. (1986): Computation of the fractal dimension of topographic surfaces using the triangular prism surface area method, *Comput. Geosci.*, **12** (5), 713-722.

CREUTZBURG, R. and E. IVANOV (1989): Fast algorithm for computing fractal dimensions of image segments, in *Recent Issues in Pattern Analysis and Recognition*, Lecture Notes in Computer Geosciences, (Springer-Verlag, Heidelberg-New York), No. 399.

DUBUC, B., J.F QUINIOU, C. ROQUES-CARMES, C. TRICOT and S.W. ZUCKER (1989): Evaluating the fractal dimension of profiles, *Phys. Rev.*, **39** (3), 1500-1521.

FEDER, J. (1988): *Fractals* (Plenum Press, New York), pp. 283.

HERZFELD, U.C., I.I. KIM, J.A. ORCUTT and C.G. FOX (1993): Fractal geometry and seafloor topography: theoretical concepts *versus* data analysis for the Juan de Fuca Ridge and the Eastern Pacific Rise, *Ann. Geophysicae*, **11**, 532-541.

HOUGH, S.E. (1989): On the use of spectral methods for the determination of fractal dimension, *Geophys. Res. Lett.*, **16** (7), 673-676.

KAYE, B.H. (1989): *A Random Walk Through Fractal Dimension* (VCH Verlagsgesellschaft, Weinheim), pp. 421.

KAYE, B.H. (1994): It's rough in the real world, *Phys. World*, **7** (11), 48-49.

KORVIN, G. (1992): *Fractal Models in the Earth Sciences* (Elsevier, Amsterdam), pp. 396.

JAGGI, S., D.A. QUATTROCHI and N.S.-N. LAM (1993): Implementation and operation of three fractal measurement algorithms for analysis of remote-sensing data, *Comput. Geosci.*, **19** (6), 745-767.

MANDELBROT, B.B. (1967): How long is the coast of Britain? Statistical self-similarity and fractional dimension, *Science*, **165**, 636-638.

MANDELBROT, B.B. (1983): *The Fractal Geometry of Nature* (W. Freeman and C.) pp. 468.

MANDELBROT, B.B. and J.R. WALLIS (1969): Computer experiments with fractional Gaussian noises, *Water Res.*, **5**, 228-267.

MEAKIN, P. (1991): Fractal aggregates in geophysics, *Rev. Geophys.*, **29** (3), 317-354.

PEITGEN, H.-O., H. JÜRGENS and D. SAUPE (1992): *Chaos and Fractals* (Springer-Verlag, New York), pp. 984.

PIECH, N.A. and K.R. PIECH (1990): Fingerprints and fractal terrains, *Math. Geology*, **22** (4), 457-485.

ROACH, D.E. and A.D. FOWLER (1993): Dimensionality analysis of patterns: fractal measurements, *Comput. Geosci.*, **19** (6), 849-869.

RUSS, J. (1994): *Fractal Surfaces* (Plenum Press, New York), pp. 309.

TURCOTTE, D.L. (1992): *Fractals and Chaos in Geology and Geophysics* (Cambridge Univ. Press, Cambridge), pp. 221.

(received July 29, 1996;
accepted January 27, 1997)

Appendix A. Fractal dimension and Hausdorff measure.

Given a geometrical object (*e.g.*, a curve, a surface, etc.) with topological dimension d (with $d = 1$, $d = 2$, etc., respectively), let us cover it by N d-dimensional rulers with characteristic length δ. We get:

$$N(\delta) \propto \delta^{-D} \tag{A.1}$$

(*e.g.*, Meakin, 1991, eq. (21), and Peitgen *et al.*, 1992, p. 218). If $D > d$ then the object is fractal and D is called its fractal dimension; in this sense D is a critical value (*e.g.*, Feder, 1988, p. 14). Technically D is a similarity dimension (Russ, 1994, p. 55).

Let us define the Hausdorff measure $M(\delta)$ as:

$$M(\delta) = N(\delta) \cdot \delta^d \propto \delta^{(d-D)} \tag{A.2}$$

(*e.g.*, Feder, 1988, p. 14; Peitgen *et al.*, 1992, p. 218).

This implies that the object is *not* fractal when its Hausdorff measure is finite and does not depend on δ, *i.e.*, when $D = d$. Otherwise, $M = M(\delta)$, so $M \to \infty$ for $D > d$ and $\delta \to 0$, which is the typical property of a fractal. M is defined as a *measure* because it generalizes the proper measure of the corresponding d-dimensional case, *i.e.*, for $d = 1$ it is the length $L(\delta)$ of a curve, for $d = 2$ it is the area $A(\delta)$ of a surface, and so on. When considering a fractal, M is often said *apparent* because it changes with the δ that is used (*e.g.*, *apparent* length).

In particular, for a fractal curve we have:

$$N(\delta) \propto \delta^{-D} \tag{A.1a}$$

with $1 < D \leq 2$, and

$$M(\delta) = L(\delta) \propto \delta^{(1-D)}; \tag{A.2a}$$

while for a fractal surface we can write:

$$N(\delta) \propto \delta^{-D} \tag{A.1b}$$

with $2 < D \leq 3$, and

$$M(\delta) = A(\delta) \propto \delta^{(2-D)}. \tag{A.2b}$$

Appendix B. Against the Schwarz paradox.

Consider the surface of the half cylinder of fig. 6. If R and H are its radius and height, respectively, then its area A is πRH. Divide the entire surface into $m \times n$ sectors, with a side parallel to the cylinder axis. In this simple case, each sector is characterized by the four points at the vertices of the square A, B, C and D (this is the typical way of applying TPM or RTPM). Since the central common point E will be always on the same plane containing all the other four vertices of the square, here, instead of considering the 4 triangles σ_1, σ_2, σ_3 and σ_4, we can consider just the entire square with area σ. The total surface area A is $m \times n \times \sigma$.

Straight trigonometry shows that

$$\sigma = \frac{RH}{m} \sin(\pi/n)$$

and

$$A = m \cdot n \cdot \sigma = nRH \sin(\pi/n). \tag{B.1}$$

For $n \to \infty$, $\sin(\pi/n)$ tends to π/n, therefore A becomes, as expected, πRH.

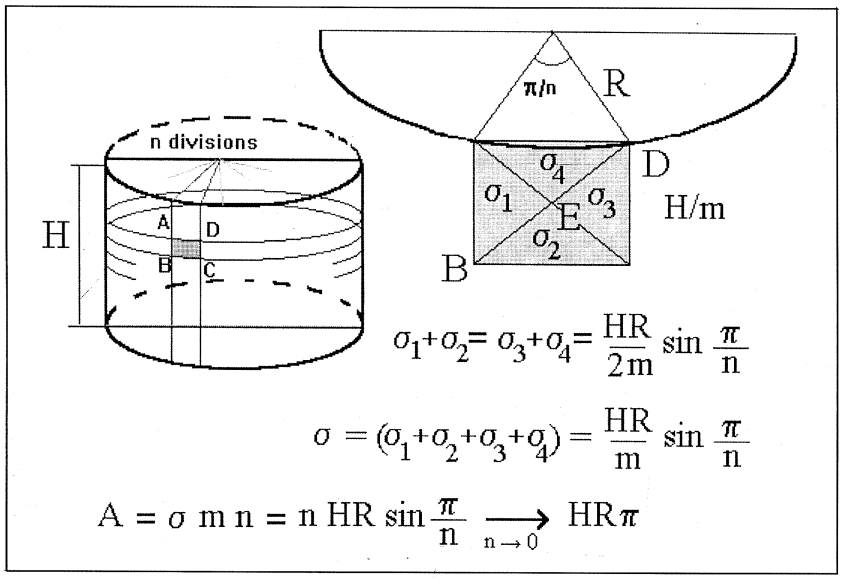

Fig. 6. Covering a cylinder to avoid Schwarz paradox. The use of an even series of triangular prisms coupled as in TPM (or RTPM) does not give the absurd results of other common triangulations.

Although for grids with other orientations with respect to the cylinder axis, the four points of each sector could be no longer in the same plane, the above described results can be generalised to any situation. This was confirmed by numerous applications of RTPM on cylindrical surfaces at different orientations and with different rulers providing always the correct dimension $D = 2$. An example is shown at the bottom of fig. 3.

The sine term in RH side of (B.1) implies the underestimation of the area of cylinders at larger rulers. This situation mimics what happens in the 1-d analogous case of circles (*e.g.*, Russ, 1994; his fig. 3 at p. 28). It is expected that this effect might generally be present, therefore it is always better to exclude larger rulers (*i.e.*, those comparable with the larger size of the analised signal) when estimating the fractal dimension with 1-d or 2-d divider methods. The possible presence of this effect could make erroneous the interpretation of the smaller and larger ruler bands of the Richardson plot in terms of structural and textural regions, respectively (*e.g.*, Kaye, 1989, p. 288).

Appendix C. Formulations for RTPM.

Let us consider the case of fig. 1a. After some simple algebra (see *e.g.*, Creutzburg and Ivanov, 1989) we have that the surface areas of the small triangular prisms σ_1, σ_2, σ_3 and σ_4 are:

$$\sigma_1 = (s/4) \cdot \sqrt{(b-a)^2 + (2e-a-b)^2 + s^2}$$

$$\sigma_2 = (s/4) \cdot \sqrt{(c-b)^2 + (2e-b-c)^2 + s^2}$$

$$\sigma_3 = (s/4) \cdot \sqrt{(d-c)^2 + (2e-c-d)^2 + s^2}$$

and

$$\sigma_4 = (s/4) \cdot \sqrt{(a-d)^2 + (2e-d-a)^2 + s^2}$$

where a, b, c, d are the z-elevations of the corresponding prism vertices A, B, C, D and e is the mean elevation (point E), *i.e.*, $e = (a+b+c+d)/4$; s is the base side of the prism.

We can now consider the value $\sigma_i = (\sigma_1 + \sigma_2 + \sigma_3 + \sigma_4)$ as the area of the i_{th} prism upper surface. Then we introduce the mean side $\delta_i = \sqrt{\sigma_i}$ for which the upper surface of the prism corresponds to the surface of a virtual square of side δ_i (fig. 1d). Consequently, we can take the mean side of each upper prism surface $\delta = < \delta_i >$ as the best estimate of the 1-d ruler (< > denotes expected value).

Hence, taking into account of (A.2b) we can write:

$$A(\delta) = N(\delta) \cdot \delta^2 \propto \delta^{(2-D)} = \delta^{\gamma}$$

or, in terms of $\sigma = \delta^2$:

$$A(\sigma) \propto \sigma^{(2-D)/2} = \sigma^{\beta} \tag{C.1}$$

since $N(\delta) \propto \delta^{-D}$ (see (A.1)).

It is straightforward to show that the fractal dimension D can be found from the slope γ of the linear part of $\log A$ *vs.* $\log \delta$ (this is the relation we used in our examples):

$$D = 2 - \gamma \tag{C.2}$$

or from the slope β of the linear part of $\log A$ *vs.* $\log \sigma$ graph:

$$D = 2(1 - \beta). \tag{C.3}$$